

# Diffusion of interacting particles in a narrow channel: The crossover from single-file to two-dimensional diffusion

D. Lucena<sup>1</sup>, D. V. Tkachenko<sup>2</sup>, K. Nelissen<sup>1,2</sup>, V. R. Misko<sup>2</sup>, W. P. Ferreira<sup>1</sup>, G. A. Farias<sup>1</sup>, and F. M. Peeters<sup>1,2</sup>

<sup>1</sup>*Departamento de Física, Universidade Federal do Ceará,*

*Caixa Postal 6030, Campus do Pici, 60455-760 Fortaleza, Ceará, Brazil*

<sup>2</sup>*Department of Physics, University of Antwerp, Groenenborgerlaan 171, B-2020 Antwerpen, Belgium*

(Dated: February 11, 2022)

Diffusive properties of a monodisperse system of interacting particles confined to a *quasi*-one-dimensional channel are studied using molecular dynamics (MD) simulations. We calculate numerically the mean-squared displacement (MSD) and investigate the influence of the width of the channel (or the strength of the confinement potential) on diffusion in channels of different shape (i.e., straight and circular). The transition (crossover) from single-file diffusion (SFD) to the two-dimensional diffusion regime is investigated. This transition, as a function of the width of the channel, is shown to change dramatically depending on the channel's confinement profile, in particular it can be either sharp (i.e., for a hard-wall confinement potential) or smooth (i.e., for a parabolic potential). This result is understood in terms of the very different distribution of the density of particles for the different confinement potentials.

PACS numbers: 82.70.Dd, 36.40.Sx, 52.27.Lw

## I. INTRODUCTION

There is a lot of theoretical and practical interest in the dynamics of systems of interacting particles in confined geometries<sup>1</sup>. Single-file diffusion (SFD) refers to a one-dimensional (1D) process where the motion of particles in a narrow channel (e.g. *quasi*-1D systems) is limited such that particles are not able to cross each other. As a consequence, the system tends to move as a whole resulting in anomalous diffusion. The mechanism of SFD was first proposed by Hodgkin and Keynes<sup>2</sup> in order to study the passage of molecules through narrow pores. Since the order of the particles is conserved over time, this results in interesting dynamics for the system, different from what is predicted from diffusion governed by Fick's law<sup>3,4</sup>. Recent advances in nanotechnology have stimulated a growing interest in SFD, in particular, the study of transport in nanopores<sup>5</sup>. Ion channels of biological membranes and carbon nanotubes<sup>6</sup> are examples of such nanopores. The macroscopic flux of particles through such nanopores is of great importance for many practical applications, e.g. particle transport across membranes is a crucial intermediate step in almost all biological and chemical engineering processes. SFD was observed in experiments on diffusion of molecules in zeolite molecular sieves<sup>7</sup>. Zeolites with unconnected parallel channels may serve as a good realization of the theoretically investigated one-dimensional systems. SFD is also related to growth phenomena<sup>8</sup>.

The theoretical background of SFD was developed in early studies on transport phenomena in 1D channels<sup>9-11</sup>. It is also interesting to learn how the size of the system will influence the diffusive properties of the system. SFD in finite size systems has been the focus of increasing attention since there are few exact theoretical results to date<sup>12-14</sup>, which showed the existence of different regimes of diffusion.

Colloidal systems, complex plasmas and vortex matter in type-II superconductors are examples of systems where SFD may occur. The use of colloidal particles is technically interesting since it allows real time and spatial direct observation of their position, which is a great advantage as compared to atoms or molecules, as shown recently in e.g. the experimental study of defect induced melting<sup>15</sup>. One typically uses micro-meter size colloidal particles in narrow channels, as shown in<sup>16,17</sup>. The paramagnetic colloidal spheres of 3.6  $\mu\text{m}$  were confined in circular trenches fabricated by photolithography and their trajectories were followed over long periods of time. Several other studies have focused on the diffusive properties of complex plasmas. A complex plasma consists of micrometer-sized ("dust") particles immersed in a gaseous plasma background. Dust particles typically acquire a negative charge of several thousand elementary charges, and thus they interact with each other through their strong electrostatic repulsion<sup>18</sup>.

Systems of particles moving in space of reduced dimensionality or submitted to an external confinement potential exhibit different behavior from their free-of-border counterparts<sup>19</sup>. The combined effect of interaction between the particles and the confinement potential plays a crucial role in their physical and chemical properties<sup>20</sup>. In Ref.<sup>21</sup>, it was found that single-file diffusion depends on the inter-particle interaction and they showed that SFD can even be suppressed if the interaction is sufficiently strong, resulting in a subdiffusive behavior slower than  $t^{0.5}$ .

In this paper, we will investigate the effects of the confinement potential on the diffusive properties of a *quasi*-1D system of interacting particles. In the limiting case of very narrow (wide) channels, particle diffusion can be referred to SFD (2D regime) characterized by subdiffusive (normal diffusive) long-time behavior  $\propto t^{0.5}$  ( $\propto t^1$ ). Here we focus on the *intermediate* regime characterized

by a transition (i.e. crossover) between the two limiting cases, where the diffusive behavior can be characterized by  $\propto t^\alpha$ , with  $0.5 < \alpha < 1$ . This intermediate regime will be studied for two different channel geometries: (i) a linear channel, and (ii) a circular channel. These two systems correspond to different experimental realizations of diffusion of charged particles in narrow channels<sup>16,22</sup>. The latter one (i.e., a circular channel) has obvious advantages: (i) it allows a long-time observation of diffusion using a relatively short circuit, and (ii) it provides constant average particle density and absence of density gradients (which occur in, e.g., a linear channel due to the entry/exit of particles in/from the channel). Thus circular narrow channels were used in diffusion experiments with colloids<sup>16</sup> and metallic charged particles (balls)<sup>23</sup>. Furthermore, using different systems allows us to demonstrate that the results obtained in our study are generic and do not depend on the specific experimental set-up.

This paper is organized as follows. In Sec. II, we introduce the model and numerical approach. In Sec. III diffusion in a system of interacting particles, confined to a straight hard-wall or parabolic channel, is studied as a function of the channel width or confinement strength. In Sec. IV, we discuss the possibility of experimental observation of the studied crossover from the SFD to 2D diffusive regime. For that purpose, we analyze diffusion in a realistic experimental set-up, i.e., diffusion of massive metallic balls embedded in a circular channel with parabolic confinement whose strength can be controlled by an applied electric field. The conclusions are presented in Sec. V.

## II. MODEL SYSTEM AND NUMERICAL APPROACH

Our model system consists of  $N$  identical charged particles interacting through a repulsive pair potential  $V_{int}(\vec{r}_{ij})$ . In this study, we used a screened Coulomb potential (Yukawa potential),  $V_{int} \propto \exp(-r/\lambda_D)/r$ . In the transverse direction, the motion of the particles is restricted either by a hard-wall or by a parabolic confinement potential. Thus the total energy of the system can be written as

$$H = \sum_{i=1}^N V_c(\vec{r}_i) + \sum_{i>j=1}^N V_{int}(\vec{r}_{ij}). \quad (1)$$

The first term of Eq. (1) represents the confinement potential, where  $V_c(\vec{r}_i)$  is given by

$$V_c(\vec{r}_i) = \begin{cases} 0 & \text{for } |y_i| \leq R_w/2 \\ \infty & \text{for } |y_i| > R_w/2, \end{cases} \quad (2)$$

for the hard-wall confinement,

$$V_c(\vec{r}_i) = \frac{1}{2}m\omega_0^2 y_i^2, \quad (3)$$

for parabolic one-dimensional potential (in the  $y$ -direction) and by

$$V_c(\vec{r}_i) = \beta(r_0 - r_i)^2, \quad (4)$$

for parabolic circular confinement. Here  $R_w$  is the width of the channel (for a hard-wall potential),  $m$  is the mass of the particles,  $\omega_0$  is the strength of the parabolic 1D confining potential,  $r_0$  is the coordinate of the minimum of the potential energy and  $r_i$  is the displacement of the  $i$ th particle from  $r_0$  (for a parabolic potential). Note that in case of a circular channel,  $r_0 = r_{ch}$ , where  $r_{ch}$  is the radius of the channel.

The second term in Eq. (1) represents the interaction potential between the particles. For the screened Coulomb potential,

$$V_{int}(\vec{r}_{ij}) = \frac{q^2}{\epsilon} \frac{e^{-|\vec{r}_i - \vec{r}_j|/\lambda_D}}{|\vec{r}_i - \vec{r}_j|}, \quad (5)$$

where  $q$  is the charge of each particle,  $\epsilon$  is the dielectric constant of the medium,  $r_{ij} = |\vec{r}_i - \vec{r}_j|$  is the distance between  $i$ th and  $j$ th particles,  $\kappa$  is the screening parameter of the potential, usually defined in terms of the screening length, and  $\lambda_D = a_0/\kappa$  is the Debye screening length with  $a_0$  the average distance between the particles. Substituting equation (5) into (1), we obtain the energy of the system  $H_Y$ :

$$H_Y = \sum_{i=1}^N V_c(\vec{r}_i) + \frac{q^2}{\epsilon} \sum_{i>j=1}^N \frac{e^{-|\vec{r}_i - \vec{r}_j|/\lambda_D}}{|\vec{r}_i - \vec{r}_j|}. \quad (6)$$

In order to reveal important parameters which characterize the system, we can rewrite the energy  $H_Y$  in a dimensionless ( $H'_Y$ ) form by making use of the following variable transformations:  $H_Y = (q^2/\epsilon a_0)H'_Y$ ,  $r = r'a_0$ , where  $a_0$  is the mean inter-particle distance in 2D. The energy of the system then becomes

$$H'_Y = \sum_{i=1}^N V'_c(\vec{r}'_i) + \sum_{i>j=1}^N \frac{e^{-\kappa|\vec{r}'_i - \vec{r}'_j|}}{|\vec{r}'_i - \vec{r}'_j|}, \quad (7)$$

and the hard-wall confinement potential is written as

$$V'_c(\vec{r}'_i) = \begin{cases} 0 & \text{for } |y'_i| \leq R'_w/2 \\ \infty & \text{for } |y'_i| > R'_w/2, \end{cases} \quad (8)$$

where  $R'_w$  is scaled by the inter-particle distance  $a_0$ . We also introduce a parameter  $\chi = (1/2)m\omega_0^2$  which is a measure for the strength of the parabolic 1D confinement potential.

For colloidal particles moving in a nonmagnetic liquid, their motion is overdamped and the stochastic Langevin equations of motion can be reduced to those for Brownian particles<sup>24</sup>:

$$\frac{d\vec{r}_i}{dt} = \frac{D_i}{k_B T} \left( \sum_{j=1}^N \frac{dV_{int}(\vec{r}_i, \vec{r}_j)}{d\vec{r}_i} + \frac{dV_c(\vec{r}_i)}{d\vec{r}_i} + \vec{F}_T^i \right). \quad (9)$$

Note, however, that in Sec. IV we will deal with massive metallic balls and therefore we will keep the inertial term in the Langevin equations of motion.

In Eq. (9),  $\vec{r}_i$ ,  $D_i$  and  $m_i$  are the position, the self-diffusion coefficient (in  $\text{m}^2/\text{s}$ ) and mass (in kg) of the  $i$ -th particle, respectively,  $t$  is the time (in seconds),  $k_B$  is the Boltzmann constant, and  $T$  is the absolute temperature of the system.  $V_{int}$  stands for the inter-particle interaction potential and  $V_c$  is the confinement potential. Finally,  $\vec{F}_T^i$  is a randomly fluctuating force, with the following properties:  $\langle \vec{F}_T \rangle = 0$  and  $\langle F_T^i(t) F_T^j(t') \rangle = 2\eta k_B T \delta_{ij} \delta(t - t')$ , which means that it is normally distributed (*i.e.* Gaussian distribution), where  $\eta$  is the friction coefficient. Equation (9) in dimensionless form is written as

$$\frac{d\vec{r}_i}{dt'} = D_i \Gamma \left( \sum_{j=1}^N \frac{dV'_{int}(\vec{r}_i, \vec{r}_j)}{d\vec{r}_i} + \frac{dV'_c(\vec{r}_i)}{d\vec{r}_i} + \vec{F}_T^i \right), \quad (10)$$

where we use the following transformation  $V_{int} = (q^2 e^{-\kappa a_0} / \epsilon a_0) V'_{int}$ ,  $D_i = D_i / a_0^2$ , and introduced a coupling parameter  $\Gamma$ , which is the ratio of the average potential energy to the average kinetic energy,  $\Gamma = \langle V \rangle / \langle K \rangle$ , such that  $\Gamma = (q^2 e^{-\kappa a_0}) / k_B T \epsilon a_0$ . The time  $t'$  is given by  $t' = tD/a_0^2$ . In what follows, we will abandon the prime ( $'$ ) notation. We have used a first order finite difference method (Euler method) to integrate Eq. (10) numerically. In case of a straight channel, periodic boundary conditions (PBC) were applied in the  $x$ -direction while in the  $y$ -direction the system is confined either by a hard-wall or by a parabolic potential. Also, we use a timestep  $\Delta t' = 0.001$  and the coupling parameter is set to  $\Gamma = 10$ . For a circular channel, we use polar coordinates  $(r, \phi)$  and model a 2D narrow channel of radius  $r_{ch}$  with parabolic potential-energy profile across the channel, *i.e.*, in the  $r$ -direction.

### III. 1D VERSUS 2D DIFFUSION IN A STRAIGHT CHANNEL

In order to characterize the diffusion of the system, we calculate the mean-squared displacement (MSD) as follows:

$$\langle \Delta x^2(t) \rangle = \frac{1}{N} \left\langle \sum_{i=1}^N [x_i(t) - x_i(0)]^2 \right\rangle_{\Delta t}, \quad (11)$$

where  $N$  is the total number of particles and  $\langle \dots \rangle_{\Delta t}$  represents the time average over a long time interval  $\Delta t$ . To keep the inter-particle distance approximately equal to unity, we defined the total number of particles for a 1D and *quasi*-1D system as

$$N = \frac{L}{\sqrt{1 - R_w^2}}; \quad R_w < 1, \quad (12)$$

where  $L$  is the size of the simulation box (in dimensionless units) in the  $x$ -direction. We have studied the system

under two different confinement potential: (i) a parabolic 1D confining potential in the  $y$ -direction, which is tunable by the strength  $\chi$  and (ii) a hard-wall confinement potential, in which particles are confined by two parallel walls separated by a distance  $R_w$ . For different values of the parabolic strength  $\chi$  and of the width of the channel  $R_w$ , we obtained the MSD curves as a function of time shown in Fig. 1(a) and Fig. 1(c), in a log-log scale. For short time scales (I), a particle does not see its neighboring particles and performs a regular random walk leading to a  $t^1$  behavior, which is followed by an intermediate stochastic regime where  $t^{\alpha_x}$  with  $0.5 < \alpha_x < 1$ . For intermediate time scales (II), there is a SFD regime which displays a sub-diffusive  $t^{\sim 0.5}$  behavior. Normal diffusion is suppressed and the SFD behavior is observed in narrow channels ( $\chi \sim 4.0$  or  $R_w \lesssim 0.50$ ), for intermediate time scale. This is due to the fact that for big (small) values of  $\chi$  ( $R_w$ ), the confinement prevents particles from passing each other. However, with decreasing  $\chi$  (increasing  $R_w$ ), as can be seen, *e.g.* for the case  $\chi = 0.25$  ( $R_w = 0.80$ ), the SFD condition turns out to be broken.

So far, we have considered the calculation of MSD taking into account only the  $x$ -direction. In order to better understand the transition from the SFD to the normal diffusion regime, we also calculated the MSD taking into account the  $y$ -direction. For this purpose, the MSD is calculated as:

$$\langle \Delta r^2(t) \rangle = \frac{1}{N} \left\langle \sum_{i=1}^N [x_i(t) - x_i(0)]^2 + [y_i(t) - y_i(0)]^2 \right\rangle_{\Delta t} \quad (13)$$

Results are shown in Fig. 1(b) and Fig. 1(d). As in the previous case, for short times there is a normal diffusion regime (I), where  $\text{MSD} \sim t^1$ , followed by a stochastic range and a single-file diffusion regime (II). For the hard-wall confinement case, however (in the SFD regime) the slope  $\alpha_r$  exhibits a reentrant behavior for  $0.20 < R_w < 0.50$ , as is seen more clearly in Fig. 2(b).

In order to understand this reentrant behavior, we have calculated the mean distance  $\langle |y| \rangle$  of the particles from the center of the channel and the standard deviation  $\sigma$ , respectively, using the probability distribution  $P(y)$ , as

$$\langle |y| \rangle = \frac{\sum_i^{N_s} |y_i| P_i(y_i)}{\sum_i^{N_s} P_i(y_i)}; \quad (14)$$

$$\sigma = \left( \frac{1}{N_s} \sum_{i=1}^{N_s} (|y_i| - \langle |y| \rangle)^2 \right)^{1/2} \quad (15)$$

where  $P(y)$  is the probability of finding a particle between  $y$  and  $y + \Delta y$ , and  $N_s$  is the total number of data points. For the ideal 1D case particles are located on a straight line. Increasing the width  $R_w$  of the confining channel will lead to a zig-zag transition<sup>18,25</sup>. This zig-zag configuration can be seen as a distorted triangular configuration in this transition zone. Different from the 1D case, the diffusion of the particles in the  $y$ -direction will, besides the confining walls, also be hindered by the

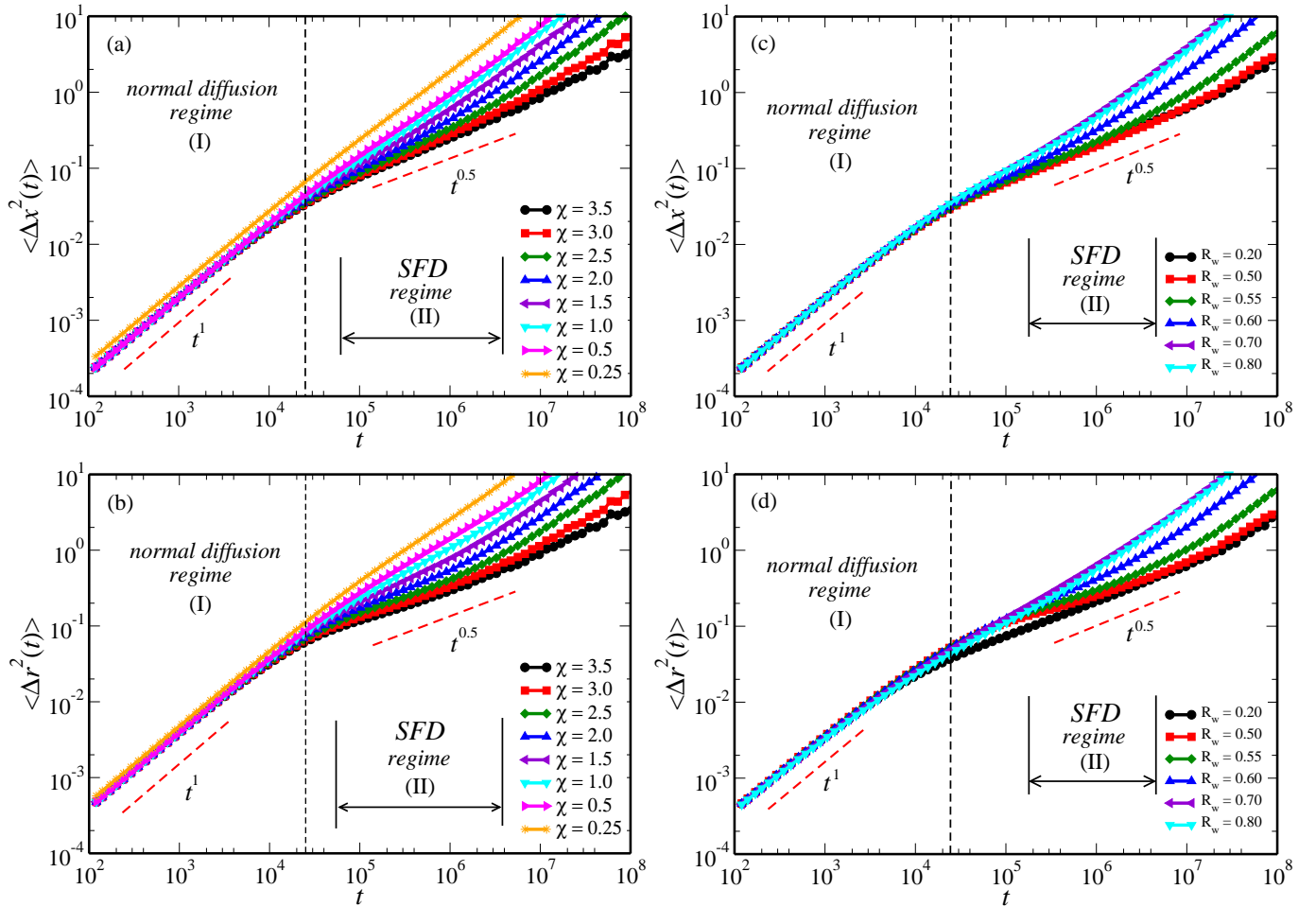


FIG. 1: (Color online) Log-log plot of the mean-squared displacement (MSD) curves as a function of time for different values of  $\chi$  (a)–(b) and of the width  $R_w$  (c)–(d) of the confining channel. Two cases are shown here: (a) and (c) MSD curves were calculated taking into account only the  $x$ -direction and (b) and (d) MSD are calculated taking into account both  $x$ - and  $y$ -directions. The red (grey) dashed lines indicate some important slopes. Two different regimes can be distinguished: normal diffusion regime and single-file diffusion (SFD) regime.

particles of the other chain, suppressing the diffusion in the  $y$ -direction, which can be seen in Fig. 3 in the range  $0.20 < R_w < 0.50$ . For  $0.50 < R_w < 0.59$ , the system is in the *quasi*-1D regime. Further increase of  $R_w$  brings the system into the 2D regime, where the normal diffusion behavior is recovered. In the  $x$ -direction, particles in different chains can overtake each other resulting in an increased  $\alpha_x$  as seen in Fig. 2(b). We have also calculated the standard deviation  $\sigma$  for different values of  $R_w$ , i.e the effective width of the particle distribution. Notice that  $\sigma$  increases with increasing  $R_w$ , as expected, since opening the channel will allow particles to move more freely. Nevertheless, for  $0.55 < R_w < 0.59$ ,  $\sigma$  remains nearly constant. This is a clear indication of the reentrant behavior: even though particles have more space to move, diffusion is suppressed. For values of  $R_w > 0.60$ , the standard deviation decreases, which indicates that the particles in the system are becoming localized in a trian-

gular lattice. Notice in Fig. 3 that the minimum in  $\alpha_r$  (Fig. 2(b)) corresponds to the maximum in the standard deviation curve.

For the parabolic 1D confinement, we can see (Fig. 5(a)) that the distribution of particles  $P(y)$  along the channel is nearly symmetric along the axis  $y = 0$ . Also, for big values of  $\chi$  (e.g.  $\chi = 3.5$ ) the particles are practically confined to move only in the  $x$ -direction, forming a single-chain structure. As the confinement is decreased ( $\chi \rightarrow 0$ ), particles tend to occupy more regions in the channel and can finally pass from the SFD regime ( $\chi \sim 3.5$ ) to the 2D normal diffusion regime ( $\chi \sim 0.5$ ). Notice that for small values of  $\chi$  (e.g.  $\chi = 0.5$ ), the system is forming a two-chain structure (Fig. 5(a)) (represented by two small peaks at the borders of the distribution  $P(y)$ ), thus allowing particles to pass each other.

The  $R_w$ -dependence of  $\alpha_r$  indicates that for a small channel width the geometrical constraint imposes the

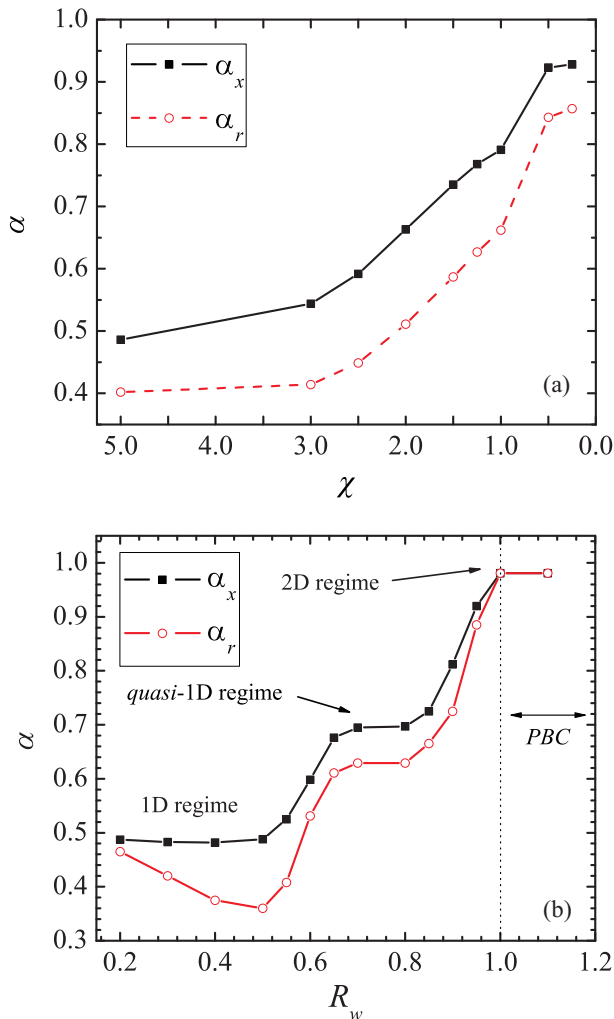


FIG. 2: (Color online) The slopes  $\alpha_x$  and  $\alpha_r$  versus (a) the strength of the parabolic 1D confinement potential  $\chi$  and (b) the width  $R_w$  of the channel in the single-file diffusion (SFD) regime (II in Fig. 1). “PBC” in (b) indicates simulations using periodic boundary conditions in both  $x$ - and  $y$ -directions.

SFD regime. As  $R_w$  increases, it is expected that the particles become more free to move along the  $y$ -direction than in the  $x$ -direction, and up to some limit, the inter-particle interaction prevents particles from overtaking each other thus imposing the SFD regime. However, Fig. 2(b) shows that  $\alpha_r$  initially decreases with increasing  $R_w$ . In order to explain this behavior, we have calculated the mean absolute value of the  $y$ -particle positions  $\langle |y| \rangle$  according to Eq. (13) and the standard deviation  $\sigma$  from it as a function of  $R_w$  (Fig. 3). The quantity  $\langle |y| \rangle$  increases continuously with  $R_w$ , suggesting that a two-chain structure starts to be formed even for small channel widths. However, for small values of  $R_w$  (e.g.  $R_w = 0.20$ ), the distribution of particles  $P(y)$  along the  $y$ -direction shows that the particles move effectively as a single-chain structure (Fig. 4(a)/Fig. 5(b)). In this case, the particle density oscillations along the

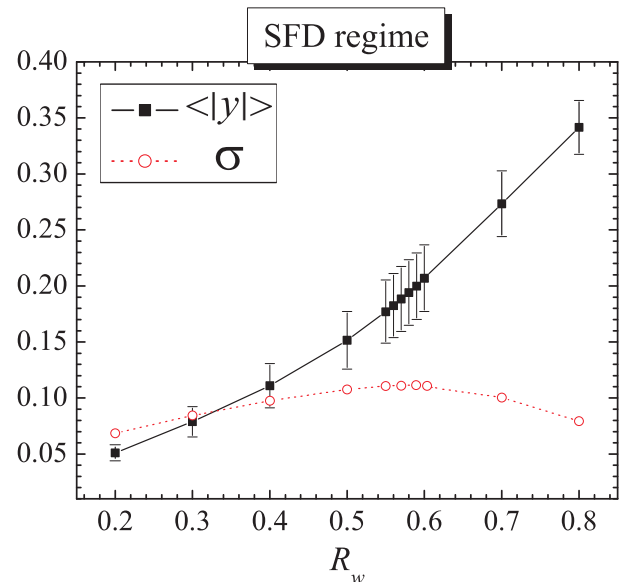


FIG. 3: (Color online) Mean absolute position  $\langle |y| \rangle$  and standard deviation  $\sigma$  as a function of the width  $R_w$  of the channel.

$y$ -direction are spread over the width of the channel, as can be seen for  $R_w = 0.20$  (Fig. 4(a)/Fig. 5(b)). Another proof of this behavior can be found in the standard deviation of  $\langle |y| \rangle$ ,  $\sigma$ , which increases with increasing  $R_w$  until  $R_w = 0.50$ . For  $R_w < 0.50$ , the SFD regime is observed, since  $\alpha \approx 0.5$ . For  $R_w > 0.50$ ,  $\sigma$  decreases with increasing  $R_w$ . This fact, together with the monotonic increase of  $\langle |y| \rangle$  as a function of  $R_w$ , shows that the two-chain structure effectively appears for  $R_w > 0.50$  (see e.g. the case  $R_w = 0.60$  in Fig. 4(b)/Fig. 5(b)) due to both the repulsive interaction between the particles in opposite chains and the geometrical constraint from the edges of the channel. Notice also that  $\alpha_r > 0.5$  for  $R_w > 0.50$ , indicating that the SFD regime has been turned into a quasi-1D diffusion regime ( $0.50 < R_w < 0.65$ ). Finally, if  $R_w > 0.65$ , the channel width is large enough and the diffusive motion of particles becomes symmetrical in both the  $x$ - and  $y$ -directions leading to the 2D normal regime ( $\alpha_r \approx 1.0$ ). The fact that in the 1D regime  $\alpha \lesssim 0.5$  and in the 2D regime  $\alpha \lesssim 1.0$  is due to the inter-particle repulsive interaction<sup>21</sup>. Changing the latter by e.g. tuning  $\kappa$  and/or the particle density, will slightly change the value of  $\alpha$ .

#### IV. DIFFUSION IN A CIRCULAR CHANNEL

In the previous section, we analyzed the transition (crossover) from the SFD regime to 2D diffusion in narrow channels of increasing width. The analysis was performed for a straight channel with either hard-wall or parabolic confinement potential. However, in terms of possible experimental verification of the studied effect, one faces an obvious limitation of this model: although

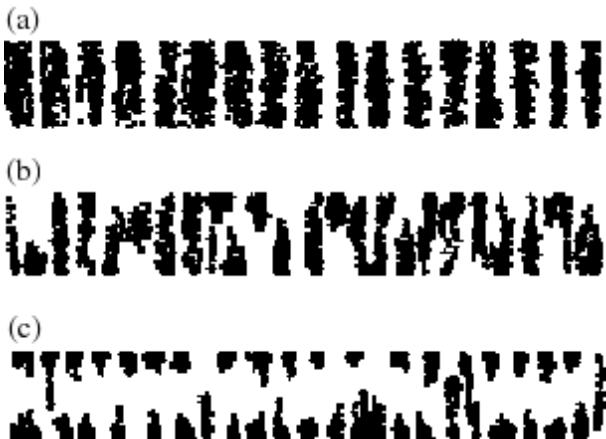


FIG. 4: For the hard-wall case, we show typical trajectories of particles (*i.e.*  $10^6$  MD simulation steps) confined by the channel of width (a)  $R_w = 0.20$ , (b)  $R_w = 0.60$  and (c)  $R_w = 0.80$ .

easy in simulation, it is hard to experimentally fulfill the periodic boundary conditions at the ends of an *open* channel. Therefore, in order to avoid this difficulty, in SFD experiments<sup>16,23</sup> circular channels were used.

In this section, we will investigate the SFD to 2D-diffusion transition (crossover) in a system of interacting particles diffusing in a channel of circular shape. In particular, we will study the influence of the strength of the confinement (*i.e.*, the depth of the potential profile across the channel) on the diffusive behavior. Without loss of generality, we will adhere to the specific conditions and parameters of the experimental set-up used in Ref.<sup>23</sup>. An additional advantage of this model is that the motion of the system of charged metallic balls<sup>23</sup> is *not* overdamped, and we will solve the full Langevin equations of motion to study the diffusive behavior of the system.

We consider  $N$  particles, interacting through a Yukawa potential (5)<sup>23</sup>, which are embedded in a ring channel of radius  $r_{ch}$ . We define a parabolic confinement potential across the channel in the form (4) where parameter  $\beta$  is chosen as follows:

$$\beta = \frac{V_0}{\gamma r_0^2}, \quad V_0 = \frac{q^2}{\epsilon} \sum_{i \neq j} \frac{\exp \left[ -2\kappa r_{ch} \sin \left( \frac{\phi_i - \phi_j}{2} \right) \right]}{2r_{ch} \sin \left( \frac{\phi_i - \phi_j}{2} \right)}, \quad (16)$$

when all the particles are equidistantly distributed along the bottom of the circular channel. It should be noted that in this case,  $V_0$  is approximately equal to  $V_{gs}$  due to the weak Yukawa interaction, which slightly shifts the particles away from the bottom of the channel. Such a choice of  $V_0$  is related to the fact that we study the influence of the confinement on the diffusion and, therefore, the potential energy of the particles must be of the order of the inter-particle interaction energy. Parameter  $r_0$  characterizes the distance when the external potential reaches the value  $V_0/\gamma$ , and  $V_{gs}$  is the energy of the

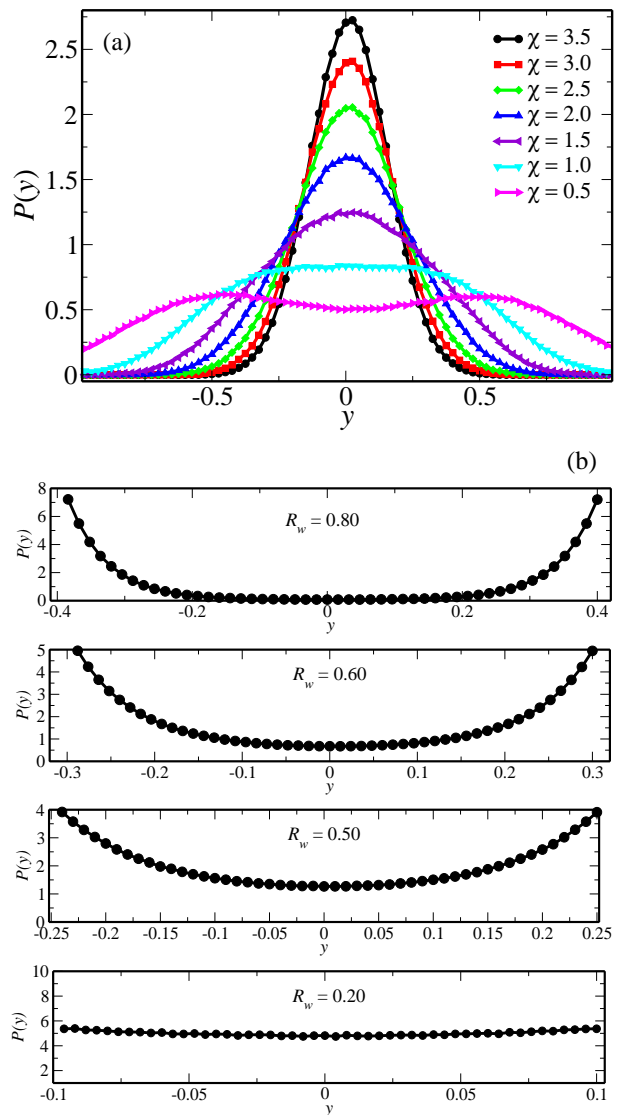


FIG. 5: (Color online) Probability distribution of the particle density  $P(y)$  along the  $y$ -direction are shown for (a) different values of  $\chi$  (parabolic 1D confinement) and (b) four different values of the width  $R_w$  of the channel (hard-wall confinement).

ground state of the system of  $N$  particles as defined by Eq. (6). Parameter  $\gamma$  plays the role of a control parameter. By changing  $\gamma$  we can manipulate the strength of the confinement and, therefore, control the fulfillment of the single-file condition. Increase in  $\gamma$  corresponds to a decrease in the depth of the confinement (4) which leads to the expansion of the area of radial localization of particles. Therefore, an increase of  $\gamma$  results in a similar effect (*i.e.*, spatial delocalization of particles) as an increase of temperature, *i.e.*, parameter  $\gamma$  can be considered as an “effective temperature”. Notice that such a choice of the parameter that controls the confinement strength is quite realistic. In the experiment of Ref.<sup>23</sup> with metallic

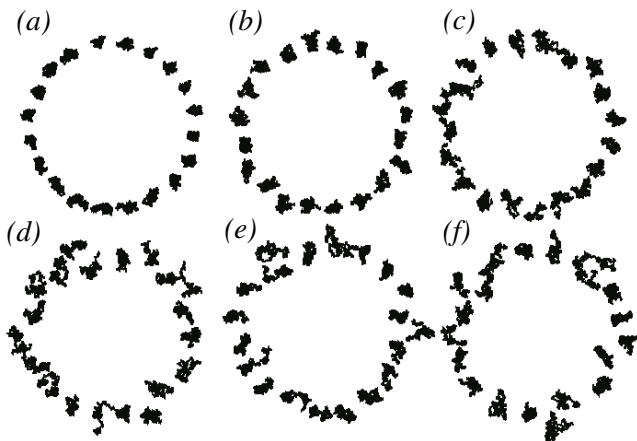


FIG. 6: Trajectories of diffusing particles for  $10^6$  consequent time steps for different values of  $\gamma$ .  $\gamma=1$  (a), 2 (b), 3 (c), 5 (d), 7 (e), 9 (f).

balls the parabolic confinement was created by an external electric field, and the depth of the potential was controlled by tuning the strength of the field.

To study diffusion of charged metallic balls, we solve the Langevin equation of motion in the general form (i.e., with the inertial term  $\propto m$ ),

$$m \frac{d^2 \vec{r}_i}{dt^2} = -\eta \frac{d\vec{r}_i}{dt} - \sum_{j, i \neq j} \vec{\nabla} V_{int}(\vec{r}_{ij}) - \vec{\nabla} V_{conf}(\vec{r}_i) + \vec{F}_T^i \quad (17)$$

where  $m = 2.5 \times 10^{-6}$  kg is the mass of a particle,  $\eta$  is the friction coefficient (inverse to the mobility). Here all the parameters of the system were chosen following the experiment<sup>23</sup>, and  $\lambda_D = 4.8 \times 10^{-4}$  m,  $\Gamma = 1$  (which is a typical experimental value, see, e.g., also<sup>16</sup>). Correspondingly, mass is measured in kg, length in m, and time in sec.

Fig. 6 shows the results of calculations of the trajectories of diffusing particles for the first  $10^6$  MD steps for various values of the parameter  $\gamma$ . As can be seen from the presented snapshots, the radial localization of particles weakens with increasing  $\gamma$ . At a certain value of  $\gamma$  this leads to the breakdown of the single-file behavior (Figs. 6(c)-(f)).

### A. Breakdown of SFD

It is convenient to introduce the distribution of the probability density of particles in the channel  $P_{rad}$  along the radial direction  $r$ . In order to calculate the function  $P_{rad}(r)$  we divided the circular channel in a number of coaxial thin rings. The ratio of the number of observations of particles in a sector of radius  $r_i$  to the total number of observations during the simulation is defined as the probability density  $P_{rad}(r_i)$ . In Fig. 7 the probability density  $P_{rad}(r)$  is presented for different values

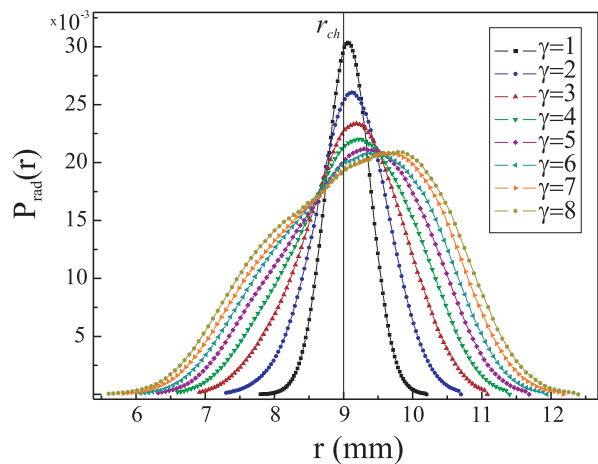


FIG. 7: (Color online) The distribution of the probability density of particles in a circular channel  $P_{rad}(r)$  along the radial direction  $r$ . The different curves correspond to various  $\gamma$ . Increasing  $\gamma$  the width of the distribution  $P_{rad}(r)$  increases due to a weakening of the confinement.

of  $\gamma$ . With increasing  $\gamma$ , the distribution of the probability density  $P_{rad}(r)$  broadens and the maximum of the function  $P_{rad}(r)$  shifts away from the center of the channel (see Fig. 7). The latter is explained by the softening of the localization of particles with increasing  $\gamma$ , which tend to occupy an area with a larger radius due to the repulsive inter-particle interaction. Simultaneously, the distribution of the probability density  $P_{rad}(r)$  acquires an additional bump indicating the nucleation of a two-channel particle distribution<sup>26</sup>. The observed broadening and deformation of the function  $P_{rad}(r)$  is indicative of a gradual increase of the probability of mutual bypass of particles (i.e., the violation of the SF condition) with increasing  $\gamma$ .

Let us now discuss a qualitative criterion for the breakdown of SFD, i.e., when the *majority* of particles leave the SFD mode. For this purpose, let us consider a particle in the potential created by its close neighbor (which is justified in case of short-range Yukawa interparticle interaction and low density of particles in a channel) shown in Fig. 8. Different lines show the interparticle potential  $V_{int}$  as a function of angle  $\phi$  for different radii  $r$ . For small values of  $\gamma$ , the maximum of the function  $P_{rad}(r)$  (see Fig. 7) coincides with that of the potential profile. Therefore, mutual passage of particles is impossible, i.e., the SF condition is fulfilled. The asymmetric broadening of the function  $P_{rad}(r)$  with increasing  $\gamma$  results in an increasing probability of mutual bypass of particles which have to overcome a barrier  $U_{bar}$  (see Fig. 8). This becomes possible when  $U_{bar} \lesssim k_B T$ . In other words, the thermal energy  $k_B T$  determines some minimal width  $\Delta r$  between adjacent particles when the breakdown of the SF condition becomes possible.

It is clear that “massive” violation of the SF condition (i.e., when the majority of particles bypass each other)

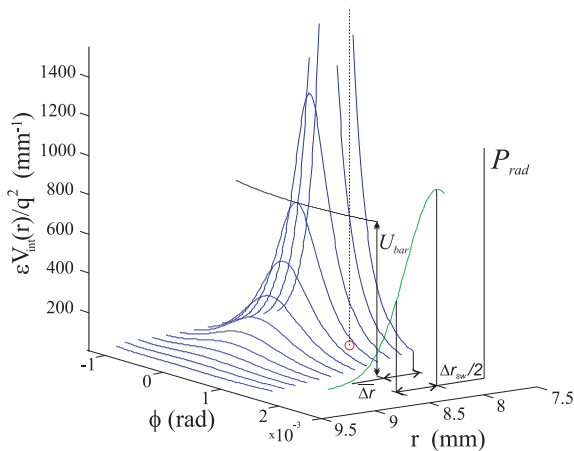


FIG. 8: (Color online) Spatial distribution of the potential  $V_{int}(r, \phi)$  created by a particle (red (grey) circle) and the qualitative distribution of the probability density of particles in circular channel  $P_{rad}(r)$  (green (light grey) line) along the radial direction  $r$ . The function  $\Delta r$  determines an approximate radial distance between particles when the potential barrier  $U_{bar}$  becomes “permeable” for given temperature  $T$ . The function  $\Delta r_{sw}$  characterizes a width of the distribution  $P_{rad}(r)$  at this temperature  $T$ .

occurs when a halfwidth  $\Delta r_{sw}$  of the distribution of the probability density  $P_{rad}(r)$  obeys the condition:

$$\Delta r_{sw} \lesssim \overline{\Delta r}. \quad (18)$$

The function  $\Delta r_{sw}$  is defined by the ratio of the thermal energy  $k_B T$  to the external potential  $U_{conf}(r)$  and is of the same order as  $\overline{\Delta r}$ :

$$\frac{V_0}{\gamma r_0^2} \cdot (\overline{\Delta r}/2)^2 \approx k_B T. \quad (19)$$

Therefore the criterion (18) can be presented in the form:

$$\Delta r_{sw} \approx \overline{\Delta r} \lesssim \overline{\Delta r}. \quad (20)$$

## B. Diffusion regimes

The MSD  $\langle \Delta \phi^2 \rangle$  is calculated as a function of time  $t$ :

$$\langle \langle \Delta \phi^2 \rangle_{ens} \rangle_{par} = \frac{1}{N_{par} N_{ens}} \sum_i \sum_j \left( \langle \Delta \phi_{i,j}^2 \rangle_t - \langle \Delta \phi_{i,j} \rangle_t^2 \right), \quad (21)$$

where  $\langle \dots \rangle_{par}$  denotes averaging over all particles of a given ensemble, and  $\langle \dots \rangle_{ens}$  denotes averaging over various ensembles. In our calculations, the number of ensembles was chosen 100 for a system consisting of 20 particles.

The time dependence of the MSD for various values of  $\gamma$  is shown in Fig. 9(a). It can be seen that for small  $\gamma$  the stochastic mode of diffusion  $\sim t$  is followed by a regime of slowing down of diffusion, which in turn is followed by

an acceleration of diffusion<sup>27</sup>. For  $\gamma > 1$  the SFD region quickly shrinks ( $\gamma = 2$ ), and then completely disappears ( $\gamma > 2$ ), being replaced by yet a subdiffusive behavior:  $\sim t^\alpha$  ( $0.5 < \alpha < 1$ ).

Fig. 9(c) shows  $\alpha$  as a function of  $\gamma$ . The function  $\alpha(\gamma)$  experiences a monotonic gradual crossover from the  $\alpha = 0.5$  to a  $\alpha \lesssim 1$ -regime. Note that the observed deviation from the normal diffusion behavior for large  $\gamma$  (Fig. 9) is related to the presence of, though weak but nonzero, external confinement in the radial direction. This change of the diffusive behavior is explained by a weakening of the average radial localization of particles with increase of  $\gamma$  (Fig. 7) and, as a consequence, by an increase of the probability of mutual bypass of particles.

The MSD-curves which take into account diffusion in both the longitudinal (angular) and transverse (radial) directions  $\langle \Delta R^2 \rangle = \langle r^2 \Delta \phi^2 \rangle + \langle \Delta r^2 \rangle$  are presented in Fig. 9(b) for different  $\gamma$ . As it is seen from Fig. 9(b) all the regimes are reproduced (i.e., the normal diffusion regime and the SFD regime) which are present in Fig. 9(a). However a similar behavior as in the case of a straight channel with parabolic confinement (see Fig. 1(b)), namely, the subdiffusive regime ( $\alpha < 0.5$ ) is observed. In other words, the qualitative modification of the diffusion curves is the same as in the case of a straight channel.

The observed crossover between the 1D single-file and 2D diffusive regimes, i.e.,  $\alpha(\gamma)$ -dependence, shows a significant different qualitative behavior as compared to the case considered in Sec. III where a rather sharp transition between the two regimes was found. The different behavior is due to the different confinement profiles and can be understood from the analysis of the distribution of the probability density of particles for these two cases. In the case of a hard-wall channel, the uncompensated (i.e., by the confinement) interparticle repulsion leads to a higher particle density near the boundaries rather than near the center of the channel. As a consequence, the breakdown of the SF condition — with increasing width of the channel — happens simultaneously for *many* particles in the vicinity of the boundary (see Fig. 3) resulting in a sharp transition (see Fig. 2(b)). On the contrary, in the case of parabolic confinement, the density distribution function has a maximum — sharp or broad, depending on the confinement strength — near the center of the channel (see Figs. 5 and 6). With increasing the “width” of the channel (i.e., weakening its strength), only a small *fraction* of particles undergoes the break down of the SF condition. This fraction gradually increases with decreasing strength of the confinement, therefore resulting in a smooth crossover between the two diffusion regimes.

## V. CONCLUSION

In conclusion, we have studied a monodisperse system of interacting particles subject to three types of confinement potentials: (i) a 1D hardwall potential, (ii) a 1D

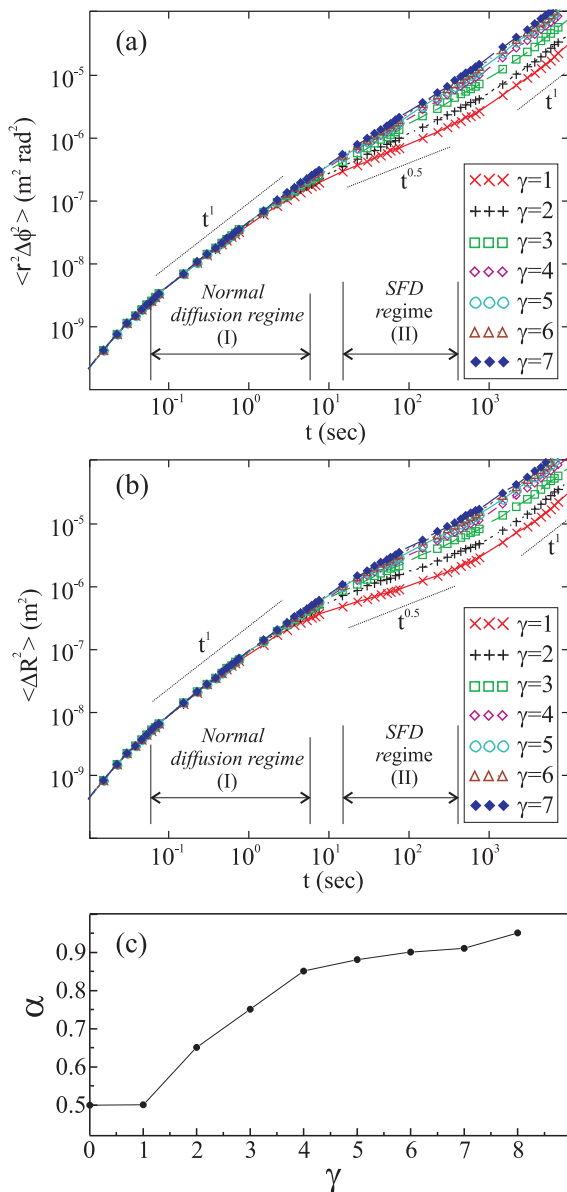


FIG. 9: (Color online) Log-log plot of the mean-squared displacement (MSD) as a function of time for different values of the “effective” temperature  $\gamma$ . MSD curves were calculated for the longitudinal direction (a) and for longitudinal and transversal directions (b). Here ( $N_{ens} = 100$ ,  $N_{par} = 20$ ). (c) The diffusion exponent  $\alpha$  as a function of  $\gamma$ . Increase of the “effective” temperature  $\gamma$  leads to the gradual transformation of the single-file regime of diffusion into the stochastic mode of diffusion of free particles.

parabolic confinement potential which both characterize a *quasi*-1D system, and (iii) a circular confining potential, which models a finite size system. In order to study

the diffusive properties of the system, we have calculated the mean-squared displacement (MSD) numerically through molecular dynamics (MD) simulations. For the case where particles were diffusing in a straight line in a Q1D channel, three diffusion regimes were found for different values of the parameters of the confining potential ( $\chi$  or  $R_w$ ), namely: a normal diffusion regime, where the MSD  $\sim t^\alpha$  with  $\alpha \sim 1$ ; a stochastic diffusion regime, which corresponds to a sub-diffusive behavior ( $t^\alpha$ , with  $0.5 < \alpha < 1$ ) and a sub-diffusive single-file diffusion regime, where  $t^\alpha$  with  $\alpha \sim 0.5$ . We have found that the normal diffusion process is suppressed if the channel width  $R_w$  is between 0.20 and 0.50 (or by  $2.0 < \chi < 3.5$ , for the case of parabolic 1D confinement), leading the system to a SFD regime for intermediate time scales. For values of  $R_w \geq 0.56$ , particles will be able to cross each other and the SFD regime will be no longer present. For the Q1D channel confined by a hardwall potential, a reentrant behavior is observed in the slope of the MSD curves for the case the mean-squared displacement is calculated for both directions ( $x$  and  $y$ ). Which means that the interparticle potential plays an important role in the diffusion properties of systems in confined geometries.

The case of a circular channel corresponds to e.g. the set-up used in experiments with sub-millimetric metallic massive balls diffusing in a ring with a parabolic potential profile created by an external electric field. The strength of the potential (which determines the effective “width” of the channel) can be tuned by the field strength. Contrary to the case of hard-wall confinement, a smooth crossover between the 1D single-file and the 2D diffusive regimes was observed. This behavior is explained by different profiles for the distribution of the particle density for the hard-wall and parabolic confinement profiles. In the former case, the particle density reaches its maximum near the boundaries of the channel resulting in a massive breakdown of the SF condition and thus in a sharp transition between the different diffusive regimes. In the latter case, on the contrary, the density distribution function has a maximum near the center which broadens with decreasing strength of the confinement. This results in a smooth crossover between the two diffusive regimes, *i.e.*, SFD and 2D regime.

## ACKNOWLEDGMENTS

This work was supported by CNPq, FUNCAP (Pronex grant), the “Odysseus” program of the Flemish Government, the Flemish Science Foundation (FWO-VI), the bilateral program between Flanders and Brazil, and the collaborative program CNPq - FWO-VI.

<sup>1</sup> C. Cottin-Bizonne, J.-L. Barrat, L. Bocquet, and E. Charlaix, *Nature Mater.* **2** 237 (2003).

<sup>2</sup> L. A. Hodgkin and D. R. Keynes, *J. Physiol.* **128**, 61

- (1955).
- <sup>3</sup> Jörg Kärger, Phys. Rev. A **45**, 4173 (1992).
  - <sup>4</sup> F. Martin, R. Walczak, A. Boiarski, M. Cohen, T. West, C. Cosentino, J. Shapiro, and M. Ferrari, J. Control. Release **102**, 123 (2005).
  - <sup>5</sup> P. Barrozo, A. A. Moreira, J. A. Aguiar, and J. S. Andrade Jr., Phys. Rev. B **80**, 104513 (2009).
  - <sup>6</sup> G. Hummer, J. C. Rasaiah, and J. P. Noworyta, Nature (London) **414**, 188 (2001).
  - <sup>7</sup> M. W. Meier and H. D. Olsen (Editors), *Atlas of Zeolite Structure Types* (Butterworths-Heinemann, London 1992).
  - <sup>8</sup> T. Halpin-Healy and Y. C. Zhang, Phys. Rep. **254**, 215 (1995).
  - <sup>9</sup> L. J. Lebowitz and K. J. Percus, Phys. Rev. E **155**, 122 (1967).
  - <sup>10</sup> D. G. Levitt, Phys. Rev. A **8**, 3050 (1973).
  - <sup>11</sup> P. M. Richards, Phys. Rev. B **16**, 1393 (1977).
  - <sup>12</sup> L. Lizana and T. Ambjörnsson, Phys. Rev. E **80**, 051103 (2009).
  - <sup>13</sup> V. N. Kharkyanen and Semen O. Yesylevskyy, Phys. Rev. E **80**, 031118 (2009).
  - <sup>14</sup> E. Barkai and R. Silbey, Phys. Rev. Lett. **102**, 050602 (2009).
  - <sup>15</sup> A. M. Alsayed, M. F. Islam, J. Zhang, P. J. Collings, and A. D. Yodh, Science **309**, 1207 (2005).
  - <sup>16</sup> H.-Q. Wei, C. Bechinger, and P. Leiderer, Science **287**, 625 (2000).
  - <sup>17</sup> C. Lutz, M. Kollmann, and C. Bechinger, Phys. Rev. Lett. **93**, 026001 (2004).
  - <sup>18</sup> G. Piacente, F. M. Peeters, and J. J. Betouras, Phys. Rev. E **70**, 036406 (2004).
  - <sup>19</sup> W. P. Ferreira, J. C. N. Carvalho, P. W. S. Oliveira, G. A. Farias, and F. M. Peeters, Phys. Rev. B **77**, 014112 (2008).
  - <sup>20</sup> W. Yang, K. Nelissen, M. Kong, Z. Zeng, and F. M. Peeters, Phys. Rev. E **79**, 041406 (2009).
  - <sup>21</sup> K. Nelissen, V. R. Misko, and F. M. Peeters, Europhys. Lett. **80**, 56004 (2007).
  - <sup>22</sup> B. Lin, M. Meron, B. Cui, S. A. Rice, and H. Diamant, Phys. Rev. Lett. **94**, 216001 (2005).
  - <sup>23</sup> G. Coupier, M. SaintJean, and C. Guthmann, Phys. Rev. E **73**, 031112 (2006).
  - <sup>24</sup> D. L. Ermak and J. A. McCammon, J. Chem. Phys. **69**, 1352 (1978).
  - <sup>25</sup> G. Piacente, G. Q. Hai, and F. M. Peeters, Phys. Rev. B **81**, 024108 (2010).
  - <sup>26</sup> Note that this is not a zig-zag transition: the function  $P_{rad}(r)$  still has a single maximum which is shifted from the center of the channel.
  - <sup>27</sup> D.V. Tkachenko, V.R. Misko, and F.M. Peeters, accepted in Phys. Rev. E (2010).